E11846

f 4/20...2

TWO-DIMENSIONAL FAILURE WAVES AND IGNITION FRONTS IN PREMIXED COMBUSTION

T. G. VEDARAJAN,[1] J. BUCKMASTER,[1] AND P. RONNEY[2]

[1]University of Illinois
Department of Aeronautical & Astronautical Engineering
Urbana, IL 61801, USA
[2]University of Southern California
Department of Mechanical Engineering
Los Angeles, CA 90089, USA

This paper is a continuation of our work on edge-flames in premixed combustion. An edge-flame is a two-dimensional structure constructed from a one-dimensional configuration that has two stable solutions (bistable equilibrium). Edge-flames can display wavelike behavior, advancing as ignition fronts or retreating as failure waves. Here we consider two one-dimensional configurations: twin deflagrations in a straining flow generated by the counterflow of fresh streams of mixture; and a single deflagration subject to radiation losses. The edge-flames constructed from the first configuration have positive or negative speeds, according to the value of the strain rate. But our numerical solutions strongly suggest that only positive speeds (corresponding to ignition fronts) can exist for the second configuration. We show that this phenomenon can also occur in diffusion flames when the Lewis numbers are small. And we discuss the asymptotics of the one-dimensional twin deflagration configuration, an overlooked problem from the 70s.

Introduction

An edge-flame can be defined, roughly speaking, as a flame sheet with an edge. There is a growing literature on edge-flames in non-premixed combustion (e.g., Ref. [1]) reflecting their important role. A flame spreading over a fuel bed, solid or liquid, will have an edge; edge flames are an important part of the structure of the combustion field that occurs in the burning of heterogeneous solid propellants [2]; they are a noticeable characteristic of candle flames under microgravity conditions [3]; and they must exist whenever a hole is torn in a flame-sheet by turbulent eddies, so that their behavior is relevant to the problem of lifted turbulent diffusion flames [4,5]. Important theoretical work has been pioneered by Dold and coworkers [6,7].

Edge-flames in premixed combustion have been less well studied. Indeed, there appears to be only a single theoretical treatment [8] and a single explicit experimental study [9]. Old experimental evidence of their existence [10] is noted in Ref. [8]. The present paper is a sequel to Ref. [8] and examines premixed edge-flames in two hitherto unexamined configurations.

A simple framework in which edge-flames can be constructed proceeds in the following fashion: There are certain one-dimensional combustion systems, dependent on a spatial variable x, say, for which there are multiple solutions. Of particular interest are bistable systems for which there are three solutions, two stable and one unstable, the counterflow

diffusion flame being a well-known example. Suppose the weakest (strongest) of the stable solutions has a temperature distribution $T_1(x)$ [$T_2(x)$]. $T_1(x)$ will often correspond to a quenched state, or a close approximation thereof, with values close to some background or supply temperature T_f. The maximum value of $T_2(x)$ will be close to a flame-temperature (e.g., the adiabatic flame-temperature or the Burke–Schumann flame-temperature). An unsteady two-dimensional combustion field can then be defined by an initial-value problem in the $x - z$ plane, where the boundary conditions in x are those for the one-dimensional problem, and

$$T(x, z, t) \to T_2(x), T_1(x) \text{ as } z \to +\infty, -\infty \quad (1)$$

If $T_2(x)$ is associated with a single thin reaction zone (flame-sheet) and $T_1(x)$ is associated with negligible reaction, an edge-flame is defined and the edge-flame structure either moves in the direction of decreasing z, in which case we call it an ignition front, or moves in the direction of increasing z, in which case we call it a failure wave. Here we continue the discussion of ignition fronts and failure waves in the premixed context. We discuss the situation where the one-dimensional problem is defined by a twin-flame counterflow, and we also discuss a deflagration in which multiple solutions arise because of radiation losses. Some related results on diffusion flames are briefly discussed, as is the asymptotic description of quenching for the twin-flame problem. As the latter
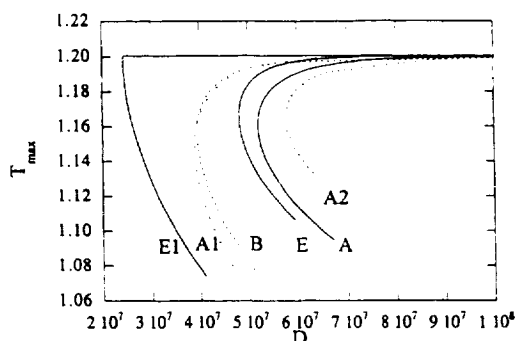
FIG. 1. Variations of maximum temperature with Damköhler number for twin counterflow flames: E, exact; E1, first-order approximation of exact solution; A, solution of the autonomous equation A10; A1, (A19), 1 term in q; A2, (A19), 2 terms in q; B, (A20).

will only be of interest to the asymptotics community, it is relegated to the Appendix.

This work and Ref. [8] are parts of the dissertation of Vedarajan [11].

The Twin-Flame Counterflow Problem

Consider a symmetric counterflow of fresh mixture that, in general, supports twin flames. This configuration has long been studied, both theoretically and experimentally.

A simple model suitable for our purposes starts with the equation

$$-\rho\alpha x d/dx(C_pT, Y) = \lambda C_p^{-1}d^2/dx^2(C_pT, Y)$$
$$+ BY \, e^{-E/RT} (Q, -1) \quad (2)$$

where α is the rate of strain and we have assumed that the Lewis number is 1. The supply conditions are

$$|x| \to \infty \quad T \to T_f, \, Y \to Y_f \quad (3)$$

If $\Delta T_a \equiv QY_f/C_p$ is used as a reference temperature, and

$$l_c \equiv \sqrt{\lambda/\rho C_p \alpha}$$

is used as a reference length, a single nondimensional equation can be deduced, namely,

$$-xT_x = T_{xx} + D(1 + T_f - T)e^{-\theta/T}, \quad (4)$$

$$D = B/\rho\alpha, \quad \theta = E/R\Delta T_a$$

Because of the symmetry, it is sufficient to solve this equation in $x > 0$ with the boundary conditions

$$T_x(0) = 0, \, T(\infty) = T_f \quad (5)$$

Note that within a context that resolves the cold-boundary difficulty (e.g., a cutoff temperature), the

system of equations 4 and 5 has a stable quenched solution in which $T = T_f$ everywhere. In addition, it is well known that for D greater than some minimum value D_{min}, there are two solutions. These can be characterized by the maximum value of T (T_{max}), and a representative response, obtained numerically, is shown as a solid line in Fig. 1 (curve E). Here $T_f = 0.2$, $T_a \equiv 1 + T_f = 1.2$, and $\theta = 16$, values adopted throughout the paper. The upper branch corresponds to stable solutions, and it is these, along with the quenched solutions, that are the key ingredients of the unsteady two-dimensional problem described in general terms in the Introduction. We are particularly concerned with solutions for values of D close to D_{min}.

As an aside, not part of the main thrust of our discussion, we note that there have been asymptotic treatments of the system of equations 2 and 3 in lieu of a numerical strategy, but there are ingredients that have not been discussed before, and we describe these in the Appendix.

Failure Waves and Ignition Waves

In this section, we use the strategy described in the Introduction to define a two-dimensional unsteady problem with $T_2(x)$ defined by a point on the upper branch of Fig. 1 (curve E) and $T_1(x) \equiv T_f$, the quenched state. The appropriate generalization of equation 4 is

$$T_t - xT_x = T_{xx} + T_{zz} + D(T_a - T)e^{-\theta/T} \quad (6)$$

now accounting for diffusion in the z direction as well as in the x direction.

Note that as $|z| \to \infty$, where $T_{zz} \to 0$, equation 6 reduces to the one-dimensional form (equation 4), and the solution $T_2(x)$ can be assigned as $z \to +\infty$, the solution $T_1(x) \equiv T_f$ as $z \to -\infty$. (Note the remark following equation 5.) Boundary conditions in x are those for the one-dimensional problem, namely, equation 5. And initial conditions, whose precise form is not important, are defined by a simple smooth interpolation between T_1 and T_2.

Figure 2a shows an initial temperature profile. Note that at $z = -5$, it is $T_1 \equiv T_f$, and at $z = +15$, it is $T_2(x)$, the one-dimensional twin-flame configuration. The Damköhler number is 4.9×10^7 and the flame sheets are merged together, because we are close to D_{min}. Figure 2b shows the profile at a later time, and it is clear that the structure is retreating, corresponding to a failure wave.

In view of the double-flame structure, it might be argued that the use of the rubric "edge-flame" is not appropriate, but the behavior revealed here has its counterpart in the edge-flames discussed in Ref. [8], where the single-flame counterflow problem is examined (fresh versus inert counterflow).

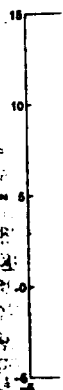If α is decreased (D increased), it is possible to

le quenched
n addition. it
me minimum
These can be
$T(T_{max})$, and
umerically, is
). Here $T_f =$
dues adopted
ranch corre-
e. along with
v ingredients
m described
We are par-
values of D

hrust of our
n asymptotic
and 3 in lieu
ingredients
and we de-

Vaves

described in
ensional un-
point on the
$(x) = T_f$, the
ralization of

$$\Gamma)e^{-\omega T} \quad (6)$$

direction as

equation 6
equation 4),
is $z \rightarrow +\infty$,
the remark
ions in x are
m, namely,
iose precise
by a simple
2.
ture profile.
it $z = +15$,
me configu-
10^7 and the
use we are
ile at a later
s retreating,

it might be
lame" is not
here has its
l in Ref. [8],
blem is ex-

possible to

FIG. 2. Temperature profiles of a failure wave $D = 4.9 \times 10^7$: (a) $t = 0$; (b) $t = 4.5$.

FIG. 3. Reaction-rate contours of an ignition front $D = 1.1 \times 10^8$, $t = 4.5$. Values are {0.5, 1.0, 3.0, 5.0, 5.0, 3.0, 1.0, 0.5}.

FIG. 4. Variations of wave speed (edge speed) with Damköhler number, twin flames.

get an ignition front. and Fig. 3 shows reaction-rate contours in such a case. Steepening of the leading (lower edge) portion of the flame is quite apparent. Here (and also for the failure wave) the front is of unchanging shape following the passage of initial transients.

By performing a number of calculations for different values of D, it is possible to construct a graph showing variations of the front speed V with D (Fig. 4). Here

$$V = (\dot{z})_+ \, S^{-1} \quad (7)$$

where $(\dot{z})_+$ is the dimensional front speed and S is the adiabatic flame speed defined by the system. The quenching value of D (D_{min}) is 4.802×10^7, and for values of D between D_{min} and D_0 (9.776×10^7), the front speed is negative. But for values of D greater than D_0, the front speed is positive. The significance of results such as these. both in the present context and in the single-flame context of Ref. [8], is that flames can experience two distinct types of quenching: global quenching, arising when D is reduced below the value D_{min}; and quenching if part of the flame has been destroyed and $D_{min} < D < D_0$ so that a failure wave enlarges the region of destruction.

Results such as these and the one-dimensional analog discussed in Ref. [8] suggest that the basic ingredients we have included here—multivaluedness, quenching—will *always* lead to the dichotomy of positive and negative speeds for the two-dimensional structure. That this is not the case is shown by the example discussed in the next section.

Multivaluedness Due to Radiation Losses

Consider the equation for a plane deflagration, radiation losses included,

$$MC_pT_x = \lambda T_{xx} + BQYe^{-E/RT} - q''' \quad (8)$$

$$q''' = 10^3\overline{MW}P_{atm} \, (Y_f - Y)(T - T_f) \, W/m^3$$

where $\overline{MW}$ is the mean molecular weight, P_{atm} is the total pressure in atmospheres. and T is the temperature in degrees Kelvin. We suppose that Y represents methane and the radiating species are CO_2 and H_2O, whose concentrations are proportional to $(Y_f - Y)$. There is a corresponding equation for Y (cf. equation
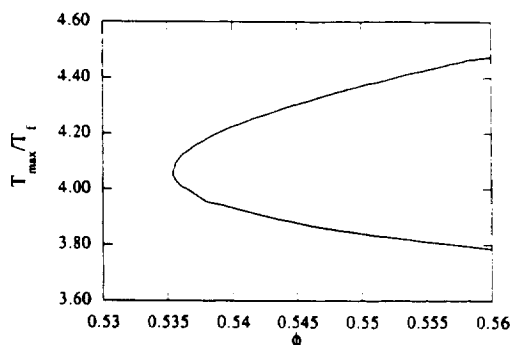
FIG. 5. Variations of flame temperature with equivalence ratio for a deflagration with radiation losses.

2). The expression for q''' is derived by first constructing an accurate representation of the temperature dependence of the band radiation for each species and then fitting this with a straight line, a surprisingly reasonable approximation up to a temperature of 1800 K. All other parameters are chosen so that the model provides a reasonable approximation of methane/air flames in the neighborhood of the lean limit. The goals are only qualitative, but we do not wish to be led astray by gross quantitative inaccuracies.

Now the system of which equation 8 is a part defines, in addition to the quenched solution $T = T_f$, $Y = Y_f$, dual solutions for values of Y_f greater than
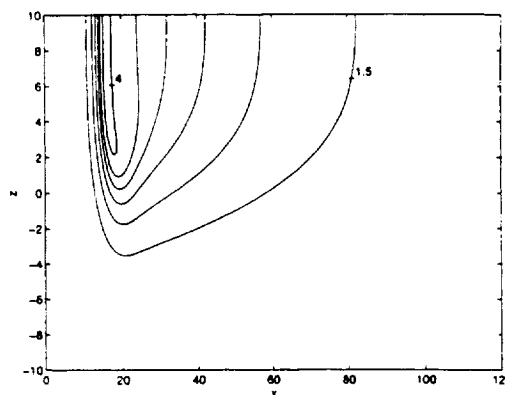

FIG. 7. Temperature contours for an ignition front with radiation losses. $\phi = 0.53556$. Values are {1.5, 2.0, 2.5, 3.0, 3.5, 4.0}.

the radiation-defined inflammability limit $Y_f = 0.02945$ (equivalence ratio $\phi = 0.5355$): See Fig. 5, the upper branch of which corresponds to stable solutions. Thus we can construct a two-dimensional unsteady combustion field (an edge-flame), and Fig. 6 shows an ignition wave for $\phi = 0.53556$, a value close to the limit. Temperature and reaction-rate contours are shown in Figs. 7 and 8. The wave is quite thick because the temperature decay occurs on a scale that is much larger than the preheat-zone thickness. Figure 9a shows variations of the
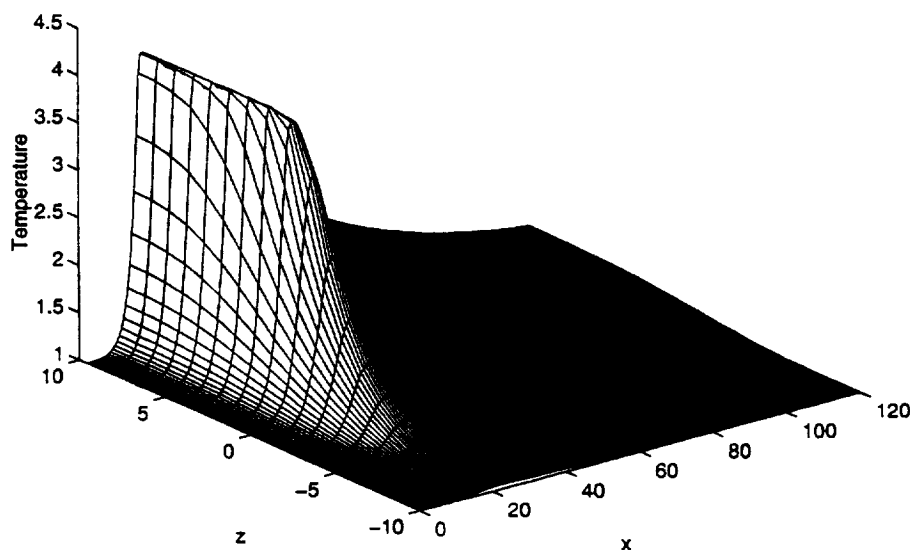

FIG. 6. An ignition front in a flame with radiation losses. $\phi = 0.53556$.

also a characteristic of existing results when the underlying one-dimensional flame is a diffusion flame (e.g., Ref. [1]).

On the other hand, if a hole is torn in a flame subject to radiation losses, the hole will heal no matter how close the equivalence ratio is to the limit value. It is natural to wonder if robust flames of this nature can occur in the counterflow configuration if the Lewis number is different from 1, and although we have no results of this nature for premixed flames, we have uncovered robust edges in the case of diffusion flames. Figure 9b shows variations of edge speed versus Damköhler number when the underlying one-dimensional flame is defined by a simple symmetric counterflow configuration (1:1 stoichiometry, both Lewis numbers equal to 0.3), and negative speeds are not obtained. However, this might not be a commonly realizable phenomenon. In examining edge-flames constructed from the S-shaped response of the Kirkby–Schmitz configuration [12] (flux conditions for the fuel applied to one boundary, Dirichlet conditions for the oxidizer applied at the other), for a variety of parameter choices, we have failed to identify robust edges even for Lewis numbers as small as 0.2.

Clearly, the results presented here and in Ref. [8] could have relevance to the behavior of turbulent premixed flames in the laminar flamelet regime, particularly where the response of turbulent flame speed to turbulent intensity "bends."

FIG. 8. Reaction-rate contours for an ignition front with radiation losses, $\phi = 0.53556$. Values are (0.04, 0.1, 0.3, ...

...speed with ϕ, results which strongly suggest negative speeds do not occur. Thus the limit equivalence ratio is 0.5355, and yet at an equivalence ratio of 0.53556, the edge speed is positive with a value approximately 0.3555. Of course, it is not possible to reduce ϕ arbitrarily close to the limit in a finite number of calculations, but it seems unlikely, as Fig. 9a is examined, that anything but positive speeds can be achieved.

Conclusions

In this paper, we have examined two examples of edge flames (but note the remark following equation ... that can arise when the reactants are premixed. The results for the symmetric (twin-flame) counterflow configuration are similar to those of the single-... configuration examined in Ref. [8]. These can be summarized by the observation that if a hole is torn in such a flame, it will get larger or smaller, depending on the value of the straining rate. This is

Appendix
Asymptotic Solution of the One-Dimensional Counterflow Problem

Here we briefly discuss the system of equations 4 and 5 in the asymptotic limit $\theta \to \infty$; there are ingredients that have not been discussed before. In the limit, reaction is confined to a flame sheet located at $x = x_*$, and if $x_* \neq 0$, we have, to first order,

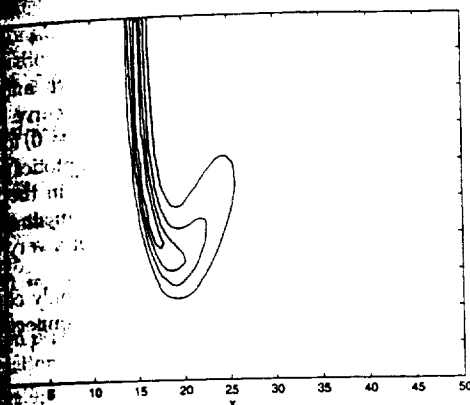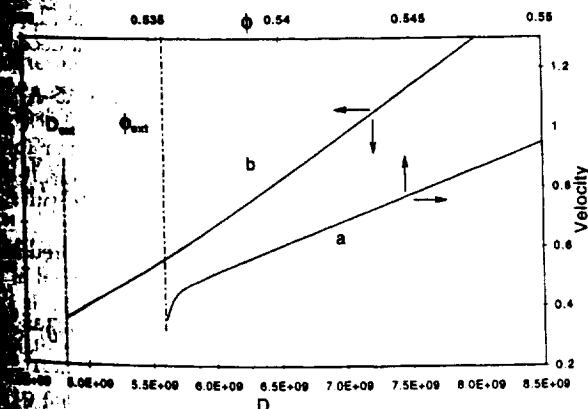
FIG. 9. Non-negative edge speeds: (a) deflagration with radiation losses and (b) symmetric diffusion counterflow configuration, $Le_X = Le_Y = 0.3$.

$$\underline{0 \le x < x_*} \quad T = 1 + T_f \equiv T_a, \quad Y = 0; \quad (A1)$$

$$\underline{x > x_*} \quad T - T_f = 1 - Y/Y_f$$

$$= \mathrm{erfc}(x/\sqrt{2})/\mathrm{erfc}(x_*/\sqrt{2})$$

The usual flame-sheet analysis determines the gradient on the unburned side of the flame,

$$Y_f^{-1} Y_x(x_* + 0) = [2DT_a^4 \theta^{-2} e^{-\theta/T_a}]^{1/2}$$

$$= \{S[\rho C_p/\alpha\lambda]^{1/2}\}_* \equiv \tilde{S} \quad (A2)$$

where S is the adiabatic flame speed defined by the system. (The label $()_*$ is used to denote a quantity that is expressed in terms of dimensional variables.) Matching with the gradient of equation A1(b) then yields a formula for x_*,

$$\sqrt{2/\pi} e^{-x_*^2/2}/\mathrm{erfc}(x_*/\sqrt{2}) = \tilde{S} \quad (A3)$$

and from this, we can deduce variations of $\tilde{x}_*$ with $\tilde{S}$, where

$$\tilde{x}_* = \{S\rho C_p \lambda^{-1} x_*\}_* = x_* \tilde{S} \quad (A4)$$

is a nondimensional flame-sheet location that is not scaled with α. $\tilde{x}_*$ decreases monotonically with increasing α, reaching the value 0 when $\tilde{S}^{-2}(\sim\alpha) = \pi/2$, a well-known result (e.g., Ref. [13]). For these solutions, the maximum temperature remains fixed at $T_a = 1 + T_f$.

There is also a solution for which $x_* = 0$ and the flame temperature T_* is within $O(1/\theta)$ of T_a. Then, to first order,

$$\underline{x > 0} \quad T = T_f + \mathrm{erfc}(x/\sqrt{2}) \quad (A5)$$

Within the reaction zone, the variables are t, ξ where

$$T = T_a(1 + \theta^{-1} T_a t), \quad x = \theta^{-1}\xi \quad (A6)$$

whence

$$t_{\xi\xi} = D\theta^{-2} e^{-\theta/T_a} t e^t \quad (A7)$$

$$t = t_*, \quad t_\xi = 0 \text{ at } \xi = 0$$

Here t_* defines the flame temperature, a quantity to be determined.

A single integration leads to

$$(t_\xi)^2 = 2D\theta^{-2} e^{-\theta/T_a} [p(t_*) - p(t)],$$

$$p(t) \equiv e^t (1 - t) \quad (A8)$$

which imposes the requirement $t \le t_* < 0$, a range in which p is an increasing function. Matching between the gradients defined by equations A5 and A8 ($x \to 0, t \to -\infty$) then leads to a formula for t_*, namely,

$$p(t_*) = 2\pi^{-1}\tilde{S}^{-2} \quad (A9)$$

defined for $\tilde{S}^{-2} < \pi/2$. This branch, with infinite slope at $\tilde{S}^{-2} = \pi/2$, is drawn in Fig. 1 (curve E1) along with the upper branch $T_* = T_a (t_* = 0)$ identified earlier when $x_* \neq 0$. Thus the asymptotics predicts a turning point (quenching point) in the response, but only provides a first-order estimate of its location ($T_* = T_a, \tilde{S}^{-2} = \pi/2$), and not a very accurate one at that.

A refinement of this description can only come from a higher-order analysis, and in this connection, we rewrite equation 4 in the form

$$T_{ss} + (\pi/2)De^{x^2} (T_a - T)e^{-\theta/T} = 0,$$

$$s = \mathrm{erf}(x/\sqrt{2}) \quad (A10)$$

Now the turning point can only be generated when at least the exponential tail of the temperature perturbation within the reaction zone interacts with the symmetry plane $x = 0$. The natural assumption is that $x_* = O(\ln\theta/\theta)$ when this occurs, corresponding to $e^{-k\xi} = O(1/\theta)$ for some k. Then we can approximate e^{x^2} by 1, and that this is a poor approximation beyond the reaction zone is obviously of no concern. Equation A10 can then be integrated using the boundary conditions

$$T_s = 0, \quad T = T_* \text{ at } s = 0 \quad (A11)$$

to yield

$$\int_{T_*}^{T} dT \, [h(-\theta/T_*) - h(-\theta/T)]^{-1/2}$$

$$= -\sqrt{\pi\theta D}s \quad (A12)$$

$$h(t) \equiv \frac{1}{2} \theta[E_i(t) - t^{-1}e^t - t^{-2}e^t]$$

$$+ T_a[E_i(t) - t^{-1}e^t]$$

where $E_i(x) = \int_{-\infty}^{x} dt \, t^{-1}e^t$ is the exponential integral. Equation A12(a), with $s = 1 (x = \infty), T = T_f$, is an implicit formula for $T_*(D)$, and this function is also plotted in Fig. 1 (curve A). It is a decent approximation to the exact solution.

If the problem implicit in Equations A5–A7 is examined to the next order, in an attempt to calculate a better approximation to the flame-temperature for the wall flame, that is, $t_* = t_{*1} + \theta^{-1} t_{*2}$, it is not difficult to show that $t_{*2} \to \infty$ as $t_{*1} \to 0$, with $t_{*2} t_{*1} \to$ const., give or take logarithmic terms. (Second-order flame-sheet theory is seldom required in our subject, but a detailed example is presented in Ref. [14].) Thus the erstwhile $1/\theta^2$ term in T_* is comparable to the $1/\theta$ term if $t_{*1} = O(1/\sqrt{\theta})$, corresponding to an $O(1/\theta\sqrt{\theta})$ deviation from T_a. The turning point is characterized by this scale.

Consider the simplified (autonomous) version of Equation A10, with the variables of equation A6. Then if the exponential is expanded,

$$d^2t/d\xi^2 = \bar{D}[te^t - T_a\theta^{-1}t^3e^t + \ldots],$$

$$\bar{D} \equiv (\pi/2)D\theta^{-2}e^{-a/T_a} \tag{A13}$$

Defining

$$q(t) = -\int_{-\infty}^{t} dt[te^t - T_a\theta^{-1}t^3e^t + \ldots] \tag{A14}$$

(then $p(t)$ is the first approximation), the solution of equation A13 satisfying the boundary conditions equation A7(b) is

$$\int_{t_*}^{t} dt\, [q(t_*) - q(t)]^{-1/2} = -\sqrt{2\bar{D}}.\xi \tag{A15}$$

with large-ξ behavior

$$t \sim -\sqrt{2\bar{D}q(t_*)}\xi + t_* + \int_{-\infty}^{t_*} dt \times$$

$$\{[1 - q(t)/q(t_*)]^{-1/2} - 1\} + \text{e.s.t.} \tag{A16}$$

Beyond the reaction zone,

$$T_{ss} = 0 \tag{A17}$$

with solution

$$T = A(\theta)s + T_f - A(\theta) \tag{A18}$$

to satisfy the boundary condition at $s = 1$, where $A(\theta)$ is a constant.

We now equate T as defined by A16 with A18 matching to all orders) so that $A = -T_a^2\sqrt{2\bar{D}q(t_*)}$ and

$$T_a^2\sqrt{2\bar{D}q(t_*)} = (T_a - T_f) + T_a^2\theta^{-1} \times$$

$$\{t_* + \int_{-\infty}^{t_*} dt\{[1 - q(t)/q(t_*)]^{-1/2} - 1\}\} \tag{A19}$$

a formula that describes variations of the flame temperature with the Damköhler number. Within the context of the autonomous problem, equation A19 is valid to all algebraic orders since an arbitrary number of terms can be retained in q.

When only the first term in $q(t)$ is retained [the term that is nominally $O(1)$], the error in t is $O(1/\theta)$, small compared to $1/\sqrt{\theta}$, and the turning point is captured, Fig. 1 (curve A1). Retaining two terms in $q(t)$ gives a better approximation, also shown in Fig. 1 (curve A2).

The term proportional to θ^{-1} in A19 plays a crucial role in defining the turning point; for at all orders, $q(0) = 0$ so that the integral is logarithmically singular as $t_* \to 0$. (That all terms in the expansion of q (equation A14) have a zero derivative at the origin means that the expansion of each q-dependent term in A19 for large θ is uniformly valid in t_*, further

justification for the validity of replacing q by its first approximation.) Indeed, for small t_* and only the first approximation for q, A19 can be approximated by

$$T_a^2\sqrt{2\bar{D}q(t_*)} \sim (T_a - T_f) + T_a^2\theta^{-1} \times$$

$$[-\sqrt{2}\ln(-t_*) + 1.34992\ldots] \tag{A20}$$

see Fig. 1 (curve B). The derivative of A20 is approximately

$$(-1/2)\sqrt{2\bar{D}}t_* + (1/\sqrt{2\bar{D}})d\bar{D}/dt_*$$

$$\sim -\sqrt{2}/(\theta t_*) \tag{A21}$$

which explicitly shows that in the immediate neighborhood of the turning point t_* is $O(1/\sqrt{\theta})$.

A final note. The formula A16 may be used to provide a measure of the overall thickness of the reaction zone (bounded on the left by the symmetry plane). The displacement effect can be calculated by finding the value of ξ for which the linear variation of t, extrapolated to small ξ, defines a value of t equal to t_*. Thus,

$$\xi_* \sim T_a^2(T_a - T_f)^{-1} \times$$

$$[-\sqrt{2}\ln(-t_*) + 1.34992\ldots] \tag{A22}$$

which is $O(\ln\theta)$ when t_* is $O(1/\sqrt{\theta})$. Recall the remarks following equation A10.

REFERENCES

1. Kioni, P. N., Rogg, B., and Bray, K. N. C., *Combust. Flame* 95:276–290 (1993).
2. Lee, S. T., Price, E., and Sigman, R., *J. Propul. Power* 10:761–768 (1995).
3. Ross, H., Sotos, R., and T'ien, J. S., *Combust. Sci. Technol.* 75:155–160 (1991).
4. Buckmaster, J., *J. Eng. Math.* 31:269–284 (1997).
5. Müller, C. M., Breitbach, H., and Peters, N., in *Twenty-Fifth Symposium (International) on Combus-*

tion, The Combustion Institute, Pittsburgh, 1994, pp. 1099–1106.

6. Dold, J. W., *Combust. Flame* 76:71–88 (1989).
7. Dold, J. W., Hartley, L. J., and Green, D., in *Dynamical Issues in Combustion Theory* (P. C. Fife, A. Liñán, and F. A. Williams, eds.) IMA Volumes in Mathematics and Its Applications, Springer, New York, 1991, pp. 83–105.
8. Vedarajan, T. G. and Buckmaster, J., *Combust. Flame* 114:267–273 (1998).
9. Jian-Bang, L. and Ronney, P. D., unpublished typescript.
10. Jarosinski, J., Strehlow, R. A., and Azarbarzin, A., in *Nineteenth Symposium (International) on Combus-*

tion, The Combustion Institute, Pittsburgh, 1982, pp. 1549–1557.

11. Vedarajan, T. G., "Edge-flames in Premixed Combustion," Ph.D. thesis, University of Illinois, Urbana, January 1998.
12. Kirkby, L. L. and Schmitz, R. A., *Combust. Flame* 10:205–220 (1966).
13. Buckmaster, J. and Ludford, G. S. S., *Lectures on Mathematical Combustion*, SIAM, Philadelphia, 1983, p. 40.
14. Buckmaster, J. and Ronney, P. in *Twenty-Seventh Symposium (International) on Combustion*, The Combustion Institute, Pittsburgh, 1998, 2603–2610.

COMMENTS

J. Chomiak, Chalmers University of Technology, Sweden. Your edge-flames are often curved. I wonder what is the mechanism of the branching phenomenon and how the branching affects the speed of the flames?

Author's Reply. The fresh/fresh counterflow edge-flame is horseshoe shaped, which is what one would expect. As for the edge-flame constructed from a deflagration with heat losses, it has only two choices: to be straight or curved, and in a two-dimensional asymmetric combustion field, it would be surprising if it were straight. The same can be said for our previous example of a premixed edge-flame, the one generated in a fresh/inert counterflow (Ref. [8] in the paper). The most obvious effect of edge curvature on the propagation speed occurs when the Lewis number (Le) is different from 1, and we will report results for premixed flames in this case elsewhere. As we briefly note for diffusion edge-flames, small values of Le lead to enhanced reaction near the edge, and the edge-speed remains positive all the way to the 1-D quenching point. Indeed, edge advancement is possible beyond the 1-D quenching point: the edge trails cellular structures, sublimit flames—obviously, it can not trail a 1-D flame. This can also happen for the deflagration-with-heat-losses problem, even if Le = 1, for reasons that we discuss elsewhere.

•

Robert Pitz, Vanderbilt University, USA. Do you expect substantial differences in your conclusions if more complex chemistry is employed in your analysis?

Author's Reply. No. The essential characteristics of unbounded edge-flames—well defined waves that can travel with positive or negative speeds, depending on the Damköhler number—have their roots in the fact that the underlying 1-D problem has two stable solutions. Whether the 1-D configuration is a diffusion flame or a premixed flame is a mere detail, as is the chemistry. Premixed failure waves (edge-flames with negative speeds) have, we believe, been seen in the sublimit failure of upward propagating methane–air flames in a standard inflammability tube, as we note in (Ref. [8] in the paper). Ronney has recently been able to establish stationary premixed edge-flames in his laboratory, and his observations are consistent with theory. These are analog-computer simulations with full chemistry. We can safely say that there are three, not two, basic flames in combustion: diffusion flames, deflagrations, and edge-flames.